

Quantum Mechanical Dynamics of Hydride Transfer in Polycyclic Hydroxy Ketones in the Condensed Phase

R. Mark Nicoll,[†] Ian H. Hillier,^{*,†} and Donald G. Truhlar[‡]

Contribution from the Department of Chemistry, University of Manchester, Manchester M13 9PL, UK, and Department of Chemistry and Supercomputer Institute, University of Minnesota, Minneapolis, Minnesota 55455

Received August 17, 2000. Revised Manuscript Received November 27, 2000

Abstract: We have used correlated electronic structure calculations and direct dynamics methods, including variational transition state theory with multidimensional semiclassical methods for calculating tunneling probabilities, to predict kinetic isotope effects (KIEs) and activation energies for hydride transfer in a polycyclic hydroxy ketone in the gas phase and aqueous solution. The need to include tunneling in the calculation of the KIEs has been shown, and the enhanced tunneling arising from a multidimensional model, compared to the one-dimensional Wigner treatment, has been demonstrated. The effect of solvent on the multidimensional tunneling contributions to the KIEs is significant and partly cancels the other contributions of the solvent to the KIEs. We also examined structural features on the kinetics for three other polycyclic hydroxy ketones by using conventional transition state theory and a Wigner tunneling approximation.

1. Introduction

Hydrogenic motion, which may be protonic, hydridic, or neutral, is an important component of the reaction coordinate in many organic, inorganic, organometallic, and enzymatic reactions.¹ Thus quantum mechanical tunneling may be important, and it is desirable to be able to model this in detail. For example, one would like to achieve a better understanding of the role of structural fluctuations in modulating enzyme-catalyzed bond cleavage involving hydrogen tunneling.² From a theoretical viewpoint the development of variational transition state theory and multidimensional semiclassical methods for calculating tunneling probabilities³ now allows a fairly accurate assessment of the relative importance of overbarrier and tunneling contributions to overall reaction rates, and the application to complicated systems is facilitated by using the direct dynamics approach.⁴ Although these theoretical treatments are computationally intensive, their use for enzyme catalysis⁵ promises a way to resolve such mechanistic problems. It is of course desirable that theoretical and experimental approaches be used together to solve these complex problems, and progress can be

made by studying suitable prototype systems. The present paper compares theory to experiment for nonenzymatic hydrogen tunneling reactions of substrate analogues in aqueous solution.

Primary kinetic isotope effects (KIEs) associated with a migrating hydrogen provide a well-established tool for characterizing transition states in many areas of mechanistic organic chemistry⁶ and enzyme catalysis,⁷ particularly where hydride transfer associated with C–H bond cleavage is involved. The use of model compounds with well-defined structure and chemical characteristics, for which experimental kinetic data are available and for which accurate theoretical interpretation of such data is feasible, should aid in understanding the factors affecting the reaction rate. An example of such an approach is the study of the kinetics of hydride transfer to NAD⁺ analogues⁸ as a model of coenzyme-mediated hydride transfer. Another interesting series of model compounds has been synthesized by Watt and co-workers, and some kinetic^{9,10} and structural data¹¹ have been obtained. These compounds are polycyclic hydroxy ketones, whose base-catalyzed rearrangements involve a hydride shift reminiscent of similar enzymatic reactions, such as the 1,2-hydride shift reaction of xylose isomerase. The model compounds of Watt et al. are exemplified by compounds I–IV shown in Figure 1. Structural data show¹¹ that bridging groups

[†] Department of Chemistry, University of Manchester.

[‡] Department of Chemistry and Supercomputer Institute, University of Minnesota.

(1) Walsh, C. *Enzymatic Reaction Mechanisms*; Freeman: San Francisco, 1979. Jordan, R. F.; Norton, J. R. *ACS Symp. Ser.* **1982**, *198*, 403–423. Goodenough, J. B. *Methods Enzymol.* **1986**, *127*, 263–284. March, J. *Advanced Organic Chemistry*, 4th ed.; Wiley: New York, 1992. Epstein, L. M.; Shubina, E. S. *Ber. Bunsen-Ges.* **1998**, *102*, 359–363. Mayer, J. E. *Acc. Chem. Res.* **1998**, *31*, 441–450. Fishbein, J. C. *Annu. Rep. Prog. Chem., Sect. B: Org. Chem.* **1999**, *95*, 265–282.

(2) Kohen, A.; Klinman, J. P. *Acc. Chem. Res.* **1998**, *31*, 397–404. Kohen, A.; Cannio, R.; Bartolucci, S.; Klinman, J. P. *Nature* **1999**, *399*, 496–499. Scrutton, N. S.; Basran, J.; Sutcliffe, M. J. *Eur. J. Biochem.* **1999**, *264*, 666–671.

(3) Truhlar, D. G.; Garrett, B. C. *Acc. Chem. Res.* **1980**, *13*, 440–448. Truhlar, D. G.; Isaacson, A. D.; Skodje, R. T.; Garrett, B. C. *J. Phys. Chem.* **1982**, *86*, 2252–2261. Truhlar, D. G.; Garrett, B. C. *Annu. Rev. Phys. Chem.* **1984**, *35*, 159–189.

(4) Truhlar, D. G.; Gordon, M. S. *Science* **1990**, *249*, 491–498. Gonzalez-Lafont, A.; Truong, T. N.; Truhlar, D. G. *J. Phys. Chem.* **1991**, *95*, 4618–4627.

(5) Alhambra, C.; Gao, J.; Corchado, J. C.; Villá, J.; Truhlar, D. G. *J. Am. Chem. Soc.* **1999**, *121*, 2253–2258. Alhambra, C.; Corchado, J. C.; Sánchez, M. L.; Gao, J.; Truhlar, D. G. *J. Am. Chem. Soc.* **2000**, *122*, 8197–8203. Nicoll, R. M.; Hindle, S. A.; MacKenzie, G.; Hillier, I. H.; Burton, N. A. *Theor. Chem. Acc.* **2000**, in press.

(6) Melander, L.; Saunders, W. H. *Reaction Rates of Isotopic Molecules*; Wiley: New York, 1980.

(7) Watt, C. I. F. In *Comprehensive Biological Catalysis*; Academic Press: New York, 1998; pp 253–272.

(8) Kreevoy, M. M.; Ostovic, D.; Truhlar, D. G.; Garrett, B. C. *J. Phys. Chem.* **1986**, *90*, 3766–3774. Kim, Y.; Truhlar, D. G.; Kreevoy, M. M. *J. Am. Chem. Soc.* **1991**, *113*, 7837–7847.

(9) Craze, G.-A.; Watt, I. *J. Chem. Soc., Perkin Trans. 2* **1981**, 175–184.

(10) Hillier, I. H.; Smith, S.; Mason, S. C.; Whittleton, S. N.; Watt, C. I. F.; Willis, J. *J. Chem. Soc., Perkin Trans. 2* **1988**, 1345–1352.

(11) Cernik, R. V.; Craze, G.-A.; Mills, O. S.; Watt, I.; Whittleton, S. N. *J. Chem. Soc., Perkin Trans. 2* **1984**, 685–690.

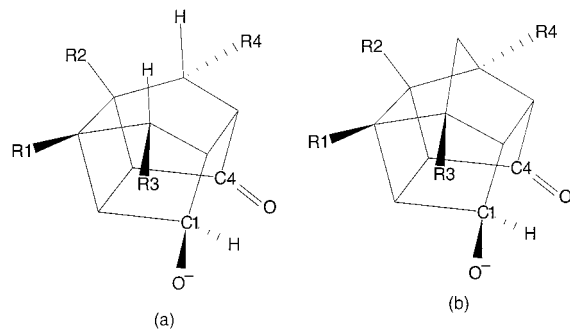


Figure 1. Structures of polycyclic hydroxy ketones: (a) **(I)** R1, R2 = H; R3, R4 = Me; **(II)** R1, R2, R3, R4 = H; **(III)** R1 = Me; R2, R3, R4 = H; (b) **(IV)** R1, R2 = H; R3, R4 = Me.

such as the methylene bridge in **IV** alter the nonbonded distance between the carbon atoms (C(1), C(4)) involved in the hydride transfer, which is reflected in quite different rates for the degenerate rearrangement occurring via 1,4-hydride shift. In addition, primary kinetic isotope data have been reported for this base-catalyzed hydride shift in compounds **I** and **III** in a mixture of water and dimethyl sulfoxide.¹⁰

One of us has previously reported *ab initio* calculations of the KIEs for the hydride shift of the unsubstituted polycyclic hydroxy ketone **II**, which by today's standards are at a very low level.¹⁰ These calculations used the Wigner one-dimensional parabolic method¹² to describe the tunneling and predicted KIEs in the range 3–5, which are somewhat larger than the experimental values. It is timely to reexamine hydride transfer in these model compounds by using high-level electronic structure methods including the effect of solvent and estimates of the reaction rate by using current direct dynamics methods.

2. Computational Details

Electronic structure calculations have been carried out on the four structurally related polycyclic hydroxy ketones shown in Figure 1. For compound **I**, calculations were carried out to identify the appropriate level of theory and basis set needed. Subsequent calculations were carried out at this level taking account of the condensed-phase environment and were further used in the direct dynamics approach to estimate kinetic quantities, in particular rate constants, activation energies, and KIEs. To model the effect of solvent we use the polarizable continuum model (PCM) of Tomasi and co-workers.¹³ Only the equilibrium electrostatic contribution to the solvation free energy was included; although cavitation, dispersion, and solvent structural effects are also important for solvation calculations,¹⁴ they are neglected here because their dependence on reaction coordinate is expected to be smaller than the electrostatic term for transfer of a charged particle. The solute cavity was taken as a superposition of atom-centered spheres having Pauling's radii. All electronic structure calculations employed the *GAUSSIAN 94* and *GAUSSIAN 98* computer programs.¹⁵

Rate constants were calculated by using semiclassical variational transition state theory (SC-VTST), which is VTST with quantized vibrational partition functions and semiclassical multidimensional tunneling contributions as implemented in the *POLYRATE* code.¹⁶ The reaction path was calculated by the method of Page and McIver¹⁷ in mass-scaled coordinates. The calculation requires generalized free energies of activation ΔG_T^{act} along the reaction path, and these in turn require vibrational partition functions. The Hessians that are needed for this step render such VTST calculations computationally expensive. Although these calculations are generally feasible for quite large systems with semiempirical Hamiltonians such as AM1 and PM3,¹⁸ they may be computationally prohibitive for even quite small systems when high

levels of theory are employed. For this reason the so-called dual-level approach is often used where information on full pathways computed at a lower level of theory is corrected by more limited information from higher level calculations, such as that relating to stationary points.¹⁹ The maximum in the generalized free energy of activation as a function of the reaction coordinate is then located and used to calculate the rate constant by canonical variational-transition-state theory (CVT). The CVT rate constants are combined with semiclassical tunneling calculations that account for quantum mechanical motions in the reaction coordinate. Models that include the effect of corner-cutting tunneling by either small-curvature tunneling (SCT) or large-curvature tunneling (LCT) paths have been developed,^{20–22} and both have been studied here, where they are compared to the results using the Wigner (W) one-dimensional parabolic¹² method and the zero-curvature-tunneling^{3,23} (ZCT) method. The rate constant $k(T)$ obtained by such calculations is finally calculated by using

$$k(T) = (\kappa k_B T/h) \exp(-\Delta G_T^{\text{CVT}}/RT) \quad (1)$$

where ΔG_T^{CVT} is the CVT free energy of activation, κ is a transmission coefficient based on the semiclassical tunneling calculation, k_B is Boltzmann's constant, T is temperature, h is Planck's constant, and R is the gas constant.

In the liquid phase, the sum of the gas-phase potential energy and the electrostatic equilibrium free energy of solvation was taken as a potential of mean force for solute motion, and the transmission coefficients were evaluated by employing the zero-order canonical-mean-shape approximation.²⁴

3. Computational Results

Structure and Energetics. We have first studied compound **I** in the absence of solvent at a number of levels of theory, the results being summarized in Table 1. In the table, HF denotes Hartree–Fock,²⁵ MP2 denotes Møller–Plesset second-order

(15) Frisch, M. J.; Trucks, G. W.; Schlegel, H. B.; Gill, P. M. W.; Johnson, B. G.; Robb, M. A.; Cheeseman, J. R.; Keith, T. A.; Petersson, G. A.; Montgomery, J. A.; Raghavachari, K.; Al-Laham, M. A.; Zakrzewski, V. G.; Ortiz, J. V.; Foresman, J. B.; Cioslowski, J.; Stefanov, B. B.; Nanayakkara, A.; Challacombe, M.; Peng, C. Y.; Ayala, P. Y.; Chen, W.; Wong, M. W.; Andres, J. L.; Replogle, E. S.; Gomberts, R.; Martin, R. L.; Fox, D. J.; Binkley, J. S.; Defrees, D. J.; Baker, J.; Stewart, J. P.; Head-Gordon, M.; Gonzalez, C.; Pople, J. A. *Gaussian 94, Rev. D1*; Gaussian, Inc.: Pittsburgh, PA, 1995. Frisch, M. J.; Trucks, G. W.; Schlegel, H. B.; Scuseria, G. E.; Robb, M. A.; Cheeseman, J. R.; Zakrzewski, V. G.; Montgomery, J. A.; Stratmann, R. E.; Burant, J. C.; Dapprich, S.; Millam, J. M.; Daniels, A. D.; Kudin, K. N.; Strain, M. C.; Farkas, O.; Tomasi, J.; Barone, V.; Cossi, M.; Cammi, R.; Mennucci, B.; Pomelli, C.; Adamo, C.; Clifford, S.; Ochterski, J.; Petersson, G. A.; Ayala, P. Y.; Cui, Q.; Morokuma, K.; Malick, D. K.; Rabuck, A. D.; Raghavachari, K.; Foresman, J. B.; Cioslowski, J.; Ortiz, J. V.; Stefanov, B. B.; Liu, G.; Liashenko, A.; Piskorz, P.; Komaromi, I.; Gomperts, R.; Martin, R. L.; Fox, D. J.; Keith, T.; Al-Laham, M. A.; Peng, C. Y.; Nanayakkara, A.; Gonzalez, C.; Challacombe, M.; Gill, P. M. W.; Johnson, B. G.; Chen, W.; Wong, M. W.; Andres, J. L.; Head-Gordon, M.; Replogle, E. S.; Pople, J. A. *Gaussian 98*; Gaussian, Inc.: Pittsburgh, PA, 1998.

(16) Corchado, J. C.; Chuang, Y.-Y.; Fast, P. L.; Villa, J.; Coitino, E. L.; Hu, W.-P.; Liu, Y.-P.; Lynch, G. C.; Nguyen, K.; Jackels, C. F.; Gu, M. Z.; Rossi, I.; Clayton, S.; Melissas, V.; Steckler, R.; Garrett, B. C.; Isaacson, A. D.; Truhlar, D. G. *POLYRATE version 7.8.1*; University of Minnesota: Minneapolis, MN, 1997.

(17) Page, M.; McIver, J. W. *J. Chem. Phys.* **1987**, *88*, 922–935.

(18) Stewart, J. J. P. *Rev. Comput. Chem.* **1990**, *1*, 45–118.

(19) Hu, W.-P.; Rossi, I.; Corchado, J. C.; Truhlar, D. G. *J. Phys. Chem. A* **1997**, *101*, 6911–6921.

(20) Liu, Y.-P.; Lu, D.-H.; Gouzalez-Lafont, A.; Truhlar, D. G.; Garrett, B. C. *J. Am. Chem. Soc.* **1993**, *115*, 7806–7817.

(21) Liu, Y.-P.; Lynch, G. C.; Truong, T. N.; Lu, D.-H.; Truhlar, D. G.; Garrett, B. C. *J. Am. Chem. Soc.* **1993**, *115*, 2408–2415.

(22) Allison, T. C.; Truhlar, D. G. In *Modern Methods for Multidimensional Dynamics Computations in Chemistry*; Thompson, D. L., Ed.; World Scientific: Singapore, 1998; pp 618–712.

(23) Truhlar, D. G.; Kuppermann, A. *J. Am. Chem. Soc.* **1971**, *93*, 1840–1851. Garrett, B. C.; Truhlar, D. G. *J. Phys. Chem.* **1979**, *83*, 2921–2926.

(24) Truhlar, D. G.; Liu, Y.-P.; Schenter, G. K.; Garrett, B. C. *J. Phys. Chem.* **1994**, *98*, 8396–8405.

(12) Wigner, E. P. *Z. Phys. Chem. B* **1932**, *19*, 203. Bell, R. P. *The Tunnel Effect in Chemistry*; Chapman & Hall: London, 1980.

(13) Tomasi, J.; Persico, M. *Chem. Rev.* **1994**, *94*, 2027–2094.

(14) Cramer, C. J.; Truhlar, D. G. *Chem. Rev.* **1999**, *99*, 2161–2200.

Table 1. Calculated Barriers (ΔV^\ddagger) and Imaginary Frequency ν_{H}^\ddagger of Transition Structure for Hydride (H^-) Transfer in Compound **I**^a

level of theory	ϵ	(ΔV^\ddagger) (kcal mol ⁻¹)	ν_{H}^\ddagger (cm ⁻¹)
gas-phase			
PM3		14.6 (12.0)	996i
HF/6-31G**		21.5 (18.8)	
B3LYP/6-31G		6.4 (4.4)	730i
B3LYP/6-31G**		5.6 (3.7)	699i
B3LYP/6-311++G**		6.6	
MP2/6-31G**		5.9	
liquid-phase ^b			
PCM/B3LYP/6-31G*	46.7	11.2 (9.3)	
PCM/B3LYP/6-31G**	46.7	10.8	
PCM/B3LYP/6-31G*	78.39	11.6 (10.7)	828i

^a ΔV^\ddagger is the classical (i.e., zero-point exclusive) barrier height, and the values in parentheses include zero-point effects. ^b ϵ denotes the dielectric constant.

perturbation theory,²⁵ B3LYP denotes hybrid Hartree–Fock density functional theory with the Becke-3-parameter approach and the Lee–Yang–Parr correlation functional,²⁶ basis sets are indicated in standard notation,²⁵ and PCM/H/b denotes the use of the PCM model with gas-phase Hamiltonian H and basis set b .

It is clear that electron correlation effects are of paramount importance in determining the barrier for hydride transfer; in particular, Table 1 shows that correlation at either an MP2 or B3LYP level yields a barrier close to 6–7 kcal mol⁻¹. The semiempirical PM3 method¹⁸ gives a barrier considerably in excess of this value. At the B3LYP/6-31G* level the major change in the cage structure during the transfer of the hydride ion to C(4) from C(1) is a reduction in the C(1)–C(4) distance from 2.62 Å in the reactant structure to 2.42 Å in the transition state. In the C_s transition state, the C(1)–H distance is 1.41 Å.

The calculated gas-phase barrier height of 6–7 kcal mol⁻¹ is considerably smaller than the experimental Arrhenius activation energy of 12.2 kcal mol⁻¹ measured for hydride transfer in a mixture of water and dimethyl sulfoxide (DMSO).²⁷ Such a difference is not unexpected since a polar solvent would be expected to preferentially stabilize the reactant structure where the negative charge is localized on a single oxygen atom rather than the symmetric transition structure which has equivalent oxygen atoms. Such a conclusion is indeed borne out by the PCM calculations, using a B3LYP functional and either a 6-31G* or 6-31G** basis, where for a dielectric constant ϵ of either 46.7 (corresponding to DMSO) or 78.39 (corresponding to H₂O) the barrier is increased from the calculated gas-phase value to one close to experiment. A barrier height closer to the measured activation energy could probably be achieved by some fine adjustment of the cavity size and/or by including first-solvation-shell effects. However, one should actually compare the calculated activation energy (not the calculated barrier height) to the experimental activation energy, and calculations using the standard PCM scheme, as used here, appear to be adequate for further studies of this hydride shift reaction. Although polar solvents lead to a substantial increase in the barrier height, we find very little change in the structure of either the reactant or transition state upon solvation. The major structural changes are a small decrease and increase in C(1)–C(4) and C(4)–O(4) distances, respectively (by 0.03 Å) in the reactant structure, upon solvation by water.

(25) Hehre, W. J.; Radom, L.; Schleyer, P. v. R.; Pople, J. A. *Ab Initio Molecular Orbital Theory*; Wiley: New York, 1986.

(26) Stephens, P. J.; Devlin, F. J.; Chabalowski, C. F.; Frisch, M. J. *J. Phys. Chem.* **1994**, *98*, 11623–11627. Kohn, W.; Becke, A. D.; Parr, R. G. *J. Phys. Chem.* **1996**, *100*, 12974–12980.

(27) Watt, C. I. F. Unpublished results.

Table 2. Effect of Structural Variations on Gas-Phase Reactivity of Hydroxy Ketones (B3LYP/6-31G**)

compd ^a	C(1)–C(4) (Å)	(ΔV^\ddagger) (kcal mol ⁻¹)	ν_{H}^\ddagger (cm ⁻¹)	κ_{H}^b	$k_{\text{H}}/k_{\text{D}}^b$
I	2.62	5.6	699i	1.44	2.93
II	2.68	7.5	746i	1.52	3.19
III	2.69	7.7	756i	1.53	3.23
IV	2.75	11.8	880i	1.71	3.68

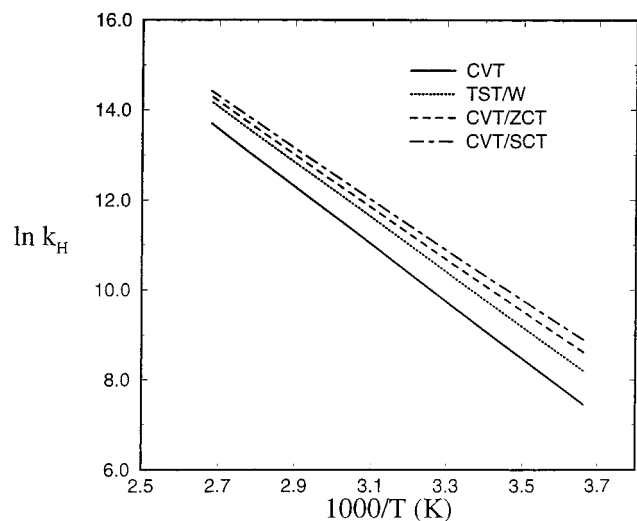
^a Figure 1. ^b Evaluated at 305 K using the Wigner tunneling factor.

Watt and co-workers have shown that the reactivity of polycyclic hydroxy ketones toward degenerate rearrangement can be substantially changed by structural modifications involving bridging methylene groups, thereby modifying the distance between the carbon atoms involving the hydride transfer. Thus, for nonbonded C(1)–C(4) distances of 2.67, 2.53, and 2.48 Å, the experimental relative reactivities are 1:10²:10³.^{9,11} We have examined this effect computationally, reporting in Table 2 the optimized C(1)–C(4) distance, together with the barrier height and imaginary harmonic frequency associated with compounds **I**–**IV**. These calculations show that the steric effect of dimethyl substitution (compound **I** relative to compound **II**) is to decrease both the C(1)–C(4) distance and the barrier, while a constraining methylene bridge (compound **IV**) increases both the C(1)–C(4) distance and the calculated barrier. A single methyl substituent (compound **III**) has little effect both on the C(1)–C(4) distance and on the calculated barrier. These calculated results are in line with the experimental data which suggest an increase in barrier height of ~4 kcal mol⁻¹ between compounds **II** and **IV**. There is also some flattening of the potential energy curve as the barrier is reduced, which has implications for tunneling through the barrier. Thus, the transmission coefficient increases somewhat for the larger barriers, with an associated increase in the kinetic isotope effect evaluated with use of the simple Wigner model (Table 2). Experimental KIEs have been reported for **I** (2.76 at 305 K) and for **III** (3.56 at 300 K).¹⁰ These values are surprisingly close to those calculated for the gas-phase reaction, using the Wigner correction for tunneling (2.93 and 3.23 for **I** and **III**, respectively). However, the calculated difference between these values is somewhat less than that reported experimentally. As part of our direct dynamical treatment of **I**, we shall discuss more detailed calculations of the reaction rate and associated KIEs.

Dynamics. All the detailed dynamics studies were carried out on compound **I**, for which kinetic data, including KIEs, are available.¹⁰ To gain some insight into the important features of the dynamics, initial calculations were carried out with use of the gas-phase PM3 potential energy surface. This approach is suggested to be useful since, although PM3 overestimates the barrier height compared to the DFT value, the value given by PM3, 12.0 kcal mol⁻¹ (Table 1), is close to the experimental activation energy observed in a mixture of water and DMSO. For this gas-phase system the minimum energy pathway (MEP) was calculated with a step size of 0.005 amu^{1/2} a₀, with Hessians being evaluated at each step. There are three transverse modes strongly coupled to the reaction coordinate: the quasisymmetric C–H–C vibration of the transferring hydride (1624 cm⁻¹), a symmetric CO stretch (1760 cm⁻¹), and an asymmetric CO stretch (1782 cm⁻¹), where the values in parentheses are evaluated at the transition state. The effect of corner cutting through these coupled modes (as well as the weakly coupled modes) is included in the SCT and LCT calculations and is reflected in the increased KIEs compared to those from the zero curvature tunneling (ZCT) model (Table 3). We find that SCT leads to a larger effect than LCT, and thus the former is used

Table 3. Calculated Gas-Phase KIEs for **I** at the PM3 Level^a

<i>T</i> (K)	CVT	CVT/W	CVT/ZCT	CVT/SCT	CVT/LCT
305	2.97	3.45	3.71	4.05	3.76
336	2.69	3.08	3.23	3.45	3.27
359	2.53	2.87	2.97	3.14	3.00

^a KIE = k_H/k_D .**Figure 2.** Arrhenius plot for gas-phase direct dynamics at the PM3 level for compound **I**. ZCT and SCT denote zero-curvature tunneling (tunneling along the MEP) and small-curvature tunneling (mild corner cutting), respectively.

in subsequent calculations; this way²⁸ of choosing the set of tunneling paths is called canonically optimized multidimensional tunneling. The rate constants calculated by various approaches are shown in Figure 2 as an Arrhenius plot. There are only small deviations from linearity, which is not very surprising for the narrow temperature range represented (275–375 K), but the increase in the rate due to tunneling is evident. For these PM3 calculations, as well as those calculations at a higher level to be described, we find that the variational transition state does not deviate significantly from the saddle point so that the rate constant calculated in the absence of tunneling will be correctly given by conventional transition state theory. We note that the gas-phase KIEs calculated in the absence of tunneling are quite close to the liquid-phase experimental values, the significant increase in the calculated values when tunneling is included leads to a definite divergence from the liquid-phase experimental values. However, we do note that as well as predicting a barrier somewhat larger than experiment, the PM3 gas-phase imaginary frequency (996i cm⁻¹) is significantly larger than that from the liquid-phase PCM calculations at the B3LYP/6-31G** level, so that the tunneling contribution to the KIEs is probably overestimated.

We now turn to estimates of the KIEs at levels of theory higher than PM3. Due to the computational expense of calculating the large number of Hessians for these medium-size systems at higher levels of theory, we have used interpolation and dual-level methods implemented within *POLYRATE*. It is, however, of interest to compare predictions of the KIEs at higher levels of theory with those from PM3. For this comparison we have taken the case of the gas-phase reaction of compound **I** at the B3LYP/6-31G level, which has both a lower barrier and a lower imaginary frequency than the PM3 case. To reduce the number

(28) Truhlar, D. G.; Lu, D.-h.; Tucker, S. C.; Zhao, X. G.; Gonzalez-Lafont, A.; Truong, T. N.; Maurice, D.; Liu, Y.-P.; Lynch, G. C. *ACS Symp. Ser.* **1992**, *502*, 16–36.

Table 4. Calculated Gas-Phase KIEs for **I** at the B3LYP/6-31G (IVTST-M) Level

<i>T</i> (K)	CVT	CVT/W	CVT/ZCT	CVT/SCT
305	2.81	3.14	2.76	2.83
336	2.56	2.82	2.53	2.58
359	2.42	2.64	2.39	2.44

Table 5. Dual-Level Calculations of the Transmission Coefficients (κ) for Hydride Transfer of Compound **I** in Water

<i>T</i> (K)	PCM/B3LYP/6-31G*/// B3LYP/6-31G(IVTST-M)			PCM/B3LYP/6-31G*/// PM3		
	W	ZCT	SCT	W	ZCT	SCT
305	1.64	1.70	2.51	1.64	2.36	2.86
336	1.52	1.54	2.09	1.52	2.01	2.33
359	1.46	1.46	1.88	1.46	1.84	2.08

of Hessians that are required, we use the interpolated variational transition state theory by mapping (IVTST-M-*H/G*) method²⁹ which evaluates gradients and Hessians at *G* and *H* points, respectively, on the MEP and interpolates between these values. Here we used IVTST-M-22/200, i.e., one Hessian every nine gradient evaluations, to be compared to a ratio of 1:2 or 1:1 used in the absence of interpolation. The results are shown in Table 4. Although the KIEs at the CVT level are only slightly reduced from those using the PM3 Hamiltonian, the KIEs at the ZCT and SCT levels are now, unlike the PM3 values, only slightly changed (<6%) from the CVT values. Such an effect has been noted previously for situations where the barrier is quite low.³⁰

It was not feasible to carry out similar calculations of the KIEs with the PCM/B3LYP MEP due to the lack of analytic second derivatives for this wave function. We thus used the dual-level approach, taking geometry, energy, and frequency information of the stationary structures at the PCM/B3LYP/6-31G* level, to correct the MEP data computed at both the PM3 and B3LYP/6-31G IVTST-M levels. Thus, with use of the nomenclature of Hu et al.,¹⁹ these calculations are designated PCM/B3LYP/6-31G*///PM3 and PCM/B3LYP/6-31G*///B3LYP/6-31G(IVTST-M), respectively.

The results of these calculations are summarized in Tables 5 and 6. We first note that the results from the two dual-level approaches are quite similar, although they use two quite dissimilar low-level potential energy surfaces, which is very encouraging as far as the credibility of the dual-level algorithm is concerned. The PM3 surface has a barrier and imaginary frequency larger than that for the high-level calculation, while the B3LYP/6-31G ($\epsilon = 1.0$) surface has a much lower barrier and imaginary frequency (Table 1). We find that both dual-level calculations predict a rate enhancement for hydrogen of ~1.5–3.0 due to tunneling, with the degree of tunneling being underestimated by the Wigner and zero-curvature models. Notice that the SCT values of the KIEs, which include corner-cutting tunneling, are 6–15% larger than ZCT values, in which tunneling paths are on the minimum-energy path. At the small-curvature level the predicted KIE falls from near 3 at 305 K to near 2.5 at 359 K. Both dual-level approaches also predict similar Arrhenius activation energies, with values close to 10 kcal mol⁻¹ when tunneling is included (Table 7).

(29) Corchado, J. C.; Coitiño, E. L.; Chuang, Y.-Y.; Fast, P. L.; Truhlar, D. G. *J. Phys. Chem. A* **1998**, *102*, 2424–2438.

(30) Storer, J. W.; Houk, K. N. *J. Am. Chem. Soc.* **1993**, *115*, 10426–10427. Hu, W.-P.; Rossi, I.; Corchado, J. C.; Truhlar, D. G. *J. Phys. Chem. A* **1997**, *101*, 6911–6921.

Table 6. Dual-Level Calculations of Kinetic Parameters for Hydride Transfer of Compound **I** in Water

T (K)	CVT	CVT/W	CVT/ZCT	CVT/SCT
PCM/B3LYP/6-31G*///B3LYP/6-31G (IVTST-M)				
rate constant (s ⁻¹)				
305	7.88E+04	1.29E+05	1.34E+05	1.98E+05
336	4.21E+05	6.42E+05	6.49E+05	8.79E+05
359	1.21E+06	1.77E+06	1.77E+06	2.28E+06
KIE				
305	2.42	2.74	2.52	2.90
336	2.24	2.49	2.31	2.57
359	2.13	2.35	2.19	2.40
PCM/B3LYP/6-31G*///PM3				
rate constant (s ⁻¹)				
305	7.88E+04	1.29E+05	1.86E+05	2.25E+05
336	4.21E+05	6.42E+05	8.47E+05	9.83E+05
359	1.21E+06	1.77E+06	2.23E+06	2.53E+06
KIE				
305	2.42	2.74	2.99	3.27
336	2.24	2.49	2.66	2.85
359	2.13	2.35	2.48	2.63

Table 7. Calculated Arrhenius Activation Energy over 305–336 K for Hydride Transfer in Compound **I**

level	CVT	CVT/W	CVT/ ZCT	CVT/ SCT
PM3	12.7	12.1	11.5	11.2
PCM/B3LYP/6-31G*///PM3	11.0	10.6	10.0	9.7
PCM/B3LYP/6-31G*/// B3LYP/6-31G (IVTST-M)	11.0	10.6	10.4	9.8

4. Discussion

We have used correlated levels of electronic structure theory and direct dynamics methods to understand the hydride transfer in some model compounds for which experimental data are available. The accuracy of variational transition state theory with optimized multidimensional tunneling, which is used here to predict rate constants, has been verified for a large number of three-body systems by comparison with accurate quantal calculations of rate coefficients.²² The systems studied here are rather more demanding cases, being quite large molecules in a condensed-phase environment.

First, we have shown that variation of the steric interactions within these polycyclic hydroxy ketones causes small, but definite variations in the distance between the carbon atoms (C(1), C(4)) involved in the hydride transfer, which can result in quite large changes in the barrier. Examination of our optimized structures shows that to form the transition state for

hydride transfer there is a reduction in the C(1)–C(4) distance of ~ 0.2 Å, the remainder of the carbon cage being essentially rigid. A polarizing environment results in a considerable increase in the barrier compared to the gas-phase value and must be included in any realistic model of the reaction. A central approximation in our work is the use of a continuum to model solvation, rather than the inclusion of explicit solvent molecules. Such an approach conveniently bypasses the problem of rigorous conformational averaging of solvent configurations but, of course, neglects explicit solvent–solute interactions. In light of this approximation, the calculated Arrhenius activation energy, within ~ 3 kcal mol⁻¹ of the experimental value, is quite satisfactory.

When combined with the potential energy surface for the hydride transfer occurring in water, calculated at the PCM level, the direct dynamics approach is very successful in understanding the origin of the measured KIEs, and the value of the dual-level approach for the study of such large systems has been demonstrated. The measurement of KIEs using tritium substitution can assist in identifying the contribution of tunneling to the KIEs,^{2,31} and it is not clear whether models involving explicit solvent may be needed to accurately help interpret such data. It is clear from the present calculations that without a tunneling correction the KIEs are definitely underestimated, values at the CVT level of 2.4–2.1 being compared to the experimental values of 2.8–2.4. Although the Wigner corrected values underestimate the tunneling correction when compared to the small-curvature values, the former are in excellent agreement with the experimental values. Thus although the calculations reported have gone a long way toward using high levels of theory to interpret the KIEs in quite complex systems, the situation is not 100% satisfactory. Various improvements could be contemplated. For example, one could explore higher levels of electronic structure theory. Also, the present treatment does not include first-solvation-shell effects or nonequilibrium solvation effects on the tunneling probabilities.³² However, these are minor quibbles. Overall the agreement of theory and experiment is encouragingly good.

Acknowledgment. We thank Dr. C. I. F. Watt for helpful discussions and EPSRC, BBSRC, and NSF for support of this research.

JA003075B

(31) Karsten, W. E.; Hwang, C.-C.; Cock, P. F. *Biochemistry* **1999**, *38*, 4398–4402.

(32) Garrett, B. C.; Schenter, G. K. *ACS Symp. Ser.* **1994**, *568*, 122–142. Chuang, Y.-Y.; Truhlar, D. G. *J. Am. Chem. Soc.* **1999**, *121*, 10157–10167.